Available online at www.eccomasproceedia.org
Eccomas Proceedia COMPDYN (2025) 1388-1398

ECCOMAS
Proceedia

COMPDYN 2025
10th ECCOMAS Thematic Conference on
Computational Methods in Structural Dynamics and Earthquake Engineering
M. Papadrakakis, M. Fragiadakis (eds.)
Rhodes Island, Greece, 15-18 June 2025

ANALYTICAL MODEL OF FRP SPIKE ANCHORS IN THE SEISMIC RESTORATION OF RC MEMBERS

Ciro Del Vecchio[1], Hothaifa A. Ali[2], Marco Di Ludovico[2], and Andrea Prota[2]

[1] Dept. of Engineering, University of Sannio
Piazza Roma, 21, 82100, Benevento, Italy
e-mail: cdelvecchio@unisannio.it

[2] Dept. of Structures for Engineering and Architecture, University of Naples Federico II
via Claudio 21, 80125, Naples, Italy
e-mail: {hothaifaabdulwahabesmail.ali, diludovi, aprota}@unina.it

Abstract

The interest in the use of FRP spike anchors is significantly increasing. This is because it has been demonstrated that they can significantly contribute to enhance the bond performance of externally bonded FRP systems and mitigate premature debonding failures under seismic loading. However, the absence of robust analytical models for practical design limits their widespread application. Current design guidelines provide minimal direction, primarily due to an incomplete understanding of the parameters governing anchor behavior. This research contributes to addressing this critical gap by presenting an analytical model capable of accurately predicting the contribution of FRP spike anchors to increase the shear capacity of FRP-strengthened beam-column joints. Key parameters such as anchor geometry, and material properties effects are incorporated to predict load-bearing capacity and failure modes. Validation against experimental demonstrates a good agreement in predicting the peak strength of anchored fabrics. A parametric analysis highlights the influence of critical variables on anchor performance, providing practical insights for optimizing design in seismic retrofitting applications. The findings contribute to advancing the understanding of FRP spike anchors' mechanical behavior and support the development of more reliable, performance-based design guidelines for seismic strengthening of RC structures.

Keywords: FRP spike anchors, seismic restoration, analytical model, bond strength, beam-column joints, CFRP quadriaxial fabrics.

ISSN:2623-3347
Peer-review under responsibility of the organizing committee of COMPDYN 2025.
doi: 10.7712/120125.12496.24517

1 INTRODUCTION

Local strengthening solutions using fiber-reinforced polymers (FRPs) have proven effective in enhancing the shear strength of beam-column joints (BCJs) and preventing premature failures, especially in post-earthquake reconstruction [1], [2], [3], [4], [5]. However, premature debonding at the FRP-concrete interface limits their performance, often requiring partial infill demolition for U-wrapping, which disrupts building functionality. To minimize such disruptions, FRP mechanical anchors have been introduced, significantly improving bond performance without extensive demolition [6], [7]. Despite promising results, the parameters influencing anchor behavior remain unclear, leading to conservative design practices due to limited guidelines. Existing empirical models lack accuracy, particularly regarding anchor quantity and placement, and no experimental studies have focused on anchored quadriaxial fabrics, which are vital for BCJ seismic strengthening. This highlights the need for a comprehensive analytical model to optimize anchor design and performance.

In this paper, existing empirical and analytical models for the FRP anchors and anchored fabrics are presented [8], [9], [10], [11], [12], [13]. These models are critically reviewed to assess their underlying assumptions, governing parameters, and applicability to different failure modes. Special attention is given to their ability to predict the contribution of FRP spike anchors in improving the tensile strength of FRP fabrics, especially in complex configurations like quadriaxial fabrics used for beam-column joint (BCJ) retrofitting.

A key focus of this study is the detailed presentation and application of the CNR DT 200 R2/2024 [8] anchor capacity model to predict the capacity of anchored quadriaxial fabric commonly used as shear strengthening of existing BCJs. This model offers updated design approaches for assessing anchor performance under seismic conditions, considering critical factors such as embedment depth, anchor spacing, concrete strength, and FRP material properties. To further evaluate the sensitivity and influence of these parameters, a parametric analysis of the CNR DT 200 R2/2024 models has been conducted. The paper explores how these models can be effectively employed in the design of local FRP strengthening strategies for exterior BCJs, where minimizing structural intervention and maximizing seismic resilience is paramount. By demonstrating the practical application of the CNR DT 200 R2/2024 guidelines, the study provides engineers with a robust framework to optimize anchor design, ensuring both reliability and efficiency in seismic retrofitting projects.

2 BACKGROUND AND LITERATURE REVIEW

Bulletin 90 [14] and Del Vecchio et al. (2015) [15] introduced an analytical model for locally strengthening exterior beam-column joints that lack shear reinforcement to increase the joint shear capacity and prevent premature shear failure in the joint. It relies on the principal stresses approach providing the design formulation to account for the contribution of the FRP strengthening to the joint principal tensile stress (see Figure 1), Eq.(1).

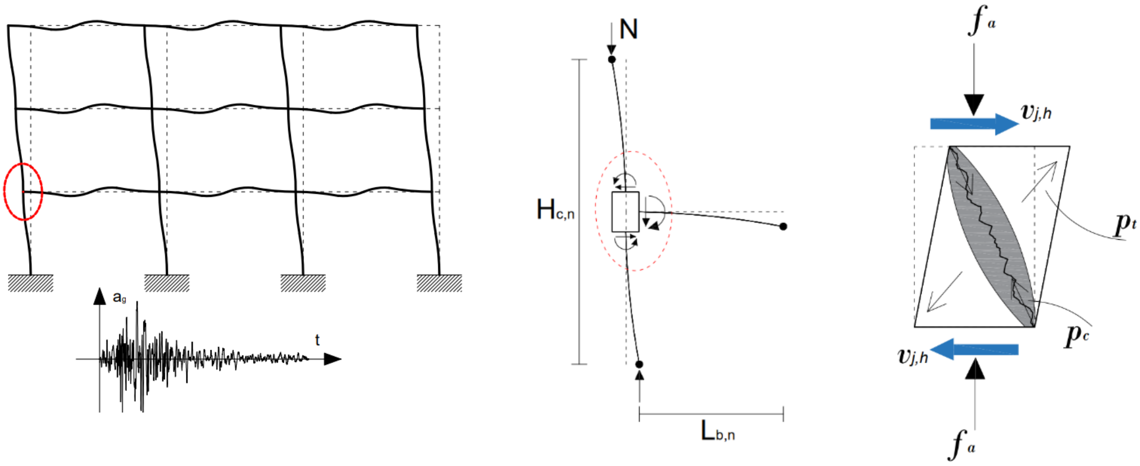

Figure 1: Beam-column joint response under seismic actions.

$$p_t = -\frac{f_a}{2} + \sqrt{\left(\frac{f_a}{2}\right)^2 + \left(v_{j,h}\right)^2} \tag{1}$$

$$p_{t,c} = 0.30\sqrt{f_{cm}} \tag{2}$$

$$p_c = \frac{f_a}{2} + \sqrt{\left(\frac{f_a}{2}\right)^2 + \left(v_{j,h}\right)^2} \leq 0.5\, f_{cm} \tag{3}$$

Where f_a represents the axial stress which is induced by the axial load on column N and $v_{i,h}$ represents the shear stress which is induced by the shear demand $V_{j,h}$. These values are calculated using ($f_a = N/A_j$) and ($v_{j,h} = V_{j,h}/A_j$), A_j represents the joint area, calculated as ($A_j = h_c * b_j$), where h_c is the effective depth of the column, and b_j is the joint width, defined as the smaller dimension between the column and beam widths.

Additionally, p_{tc} is the tensile capacity of the concrete and p_c is the diagonal compressive stress which must be limited to (0.5 * f_{cm}) to avoid concrete crushing. Furthermore, A_f is the equivalent area of the of quadriaxial CFRP fabric applied with fibers inclined in the directions inclined by 0°, 90° and ± 45°, this area is calculated using Eq.(4):

$$A_f = n_s\, t_f\, h_c\, cos\theta\ (1 + tan\theta + 2\ tan^2\theta) \tag{4}$$

The variable n_s represents the number of joint sides in each direction, and it equals one for corner exterior directions, and t_f is the thickness of each layer in the quadriaxial fabric. The angle of the principal stress, denoted by θ, can be calculated using ($\theta = \arctan(h_b/h_c)$). In these calculations, h_b and h_c refer to the effective depths of the beam and column, respectively.

The effective strain which can be developed in the fabrics is calculated using Eq.(5), where E_f is the elastic modulus of FRP fabrics

$$\varepsilon_{fd} = 34\left(\frac{f_{cm}^{2/3}}{A_f E_f}\right)^{0.6} \tag{5}$$

$$p_{t,f} = \frac{A_f\, E_f\, \varepsilon_{fd}}{b_c\,(h_c/sin\theta)} \tag{6}$$

$$p_{t,tot} = p_{t,c} + p_{t,f} \;\geq\; p_t \tag{7}$$

Where $p_{t,f}$,is the tensile capacity of the fabric in the diagonal direction. The total capacity of the joint is given by $p_{t,tot}$ in Eq.(7) and must be higher than the demand principle tensile stress p_t .

However, this approach has been calibrated considering classic end anchors such as U-wrapping at beams and column ends since no tests were available on BCJs strengthened by using spike anchors. In recent years several experimental tests were performed on BCJs strengthened with FRP fabrics anchored with FRP spike anchors. This is because this solution has the main advantage to be installed only from the exterior of the building, unlike U-wrappings which require the demolition of small portion of infills.

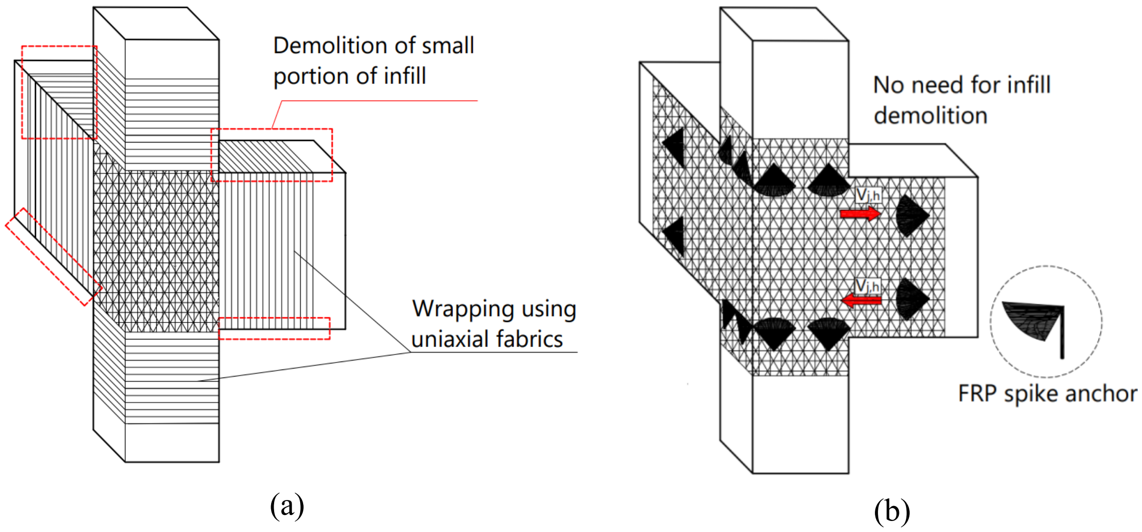

Figure 2: (a) Classical joint strengthening using U-wrapping; (b) Joint strengthening using FRP spike anchors.

2.1 Anchor capacity

Mahrenholtz [13] proposed a model that reflects the extremely low (6%) efficiency observed on the tests of the bent anchors exhibiting the fiber rupture failure mode (see Eq.(8)).

$$P_{fr} = 0.06 A_{dowel} \cdot f_{FRP} \tag{8}$$

Where P_{fr} is the anchor fiber rupture capacity, A_{dowel} is the cross-sectional area of the FRP anchor in (mm^2), and f_{FRP} is the ultimate tensile strength of the sheet used to manufacture the anchor in (MPa).

Del Rey Castillo [12], [16] proposed a model that categorizes failure modes into concrete-cone failure, combined concrete-cone and bond failure, dowel pull-out, fan-to-sheet debonding, and fiber rupture. del Rey Castillo employed the same equations developed by Kim and Smith [9] Eq.(9),(10), and (11) for cone concrete failure P_{cc} and adherent failure P_{cb}. Additionally introduced new models for pullout failure (see Eq.(12)) and fan-to-sheet debonding failure (see Eq.(13)).

- Concrete-cone failure:

$$P_{cc} = 9.68{h_{em}}^{1.5}.\sqrt{f_c} \tag{9}$$

- Combined concrete-cone and bond failure:

$$P_{cb} = 4.62\pi d_{hole} h_{em} \ \leftrightarrow \ (f_c < 20\ MPa) \tag{10}$$

$$P_{cb} = 9.07\pi d_{hole} h_{em} \ \leftrightarrow \ (f_c \geq 20\ MPa) \tag{11}$$

Where P_{cc} and P_{cb} are the anchor concrete-cone, combined concrete cone, and bond capacities in (N) respectively, h_{em} is the embedment depth (mm), f_c is the compressive strength of the concrete in (MPa), and d_{hole} is the hole diameter (mm).

- Dowel pull-out failure mode:

$$P_{po} = 0.7h_{em} - 18 \tag{12}$$

Where P_{po} is the capacity of bent anchors to resist pull-out failure in (kN) and h_{em} is the embedment depth in (mm).

- Fan-to-sheet failure mode:

$$P_{sd} = 0.35\tau_{sd}A_s \tag{13}$$

Where P_{sd} is the anchor splay debonding capacity in (N), τ_{sb} is the shear bond strength of the epoxy resin and A_s is the total area of the anchor fan bonded to the FRP sheet.

Villanueva et al. (2017) [10] adopted the same expression for the combined and anchor fracture failure that were introduced by Kim and Smith [9] and proposed the bend failure expression P_{bend} for the failure mode that exhibits the fiber rupture, which depends on the insertion angle ψ, embedment depth h_{em}, and bend ratio r_b, the equation to calculate the average tensile capacity of bent anchors exhibiting the fiber rupture failure mode is reported in Eq.(15).

$$P_{\text{anc}} = \min\left(P_{cb}, P_{bend}, P_{fr}\right) \tag{14}$$

$$P_{bend} = 0.002A_{dowel}.f_{FRP}\left(h_{em} + 50r_b\frac{\psi}{\pi}\right) \tag{15}$$

$$P_{fr} = 0.59A_{dowel}.f_{FRP} \tag{16}$$

The latest version of the Italian guidelines for FRPs in construction (CNR DT200 R2/2024) [8] presented expressions for anchor capacity with different failure modes models for FRP anchors which exhibit:

- Pull-out failure (PO): governed by embedment depth and concrete compressive strength

- Dowel sliding failure (S): governed by dowel diameter, embedded length, and concrete strength.
- Fan debonding failure (DB): related to shear bond at the fan-to-sheet interface, considering bond strength and fan length.
- Anchor rupture failure (FR): which is governed by insertion angle and fibers tensile strength.

2.2 Anchored fabric capacity

Villanueva et al. (2017) [10] proposed a conservative equation for the anchored joint capacity, which restricts the anchor's contribution to 0.58, irrespective of the anchor's capacity (see Eq.(17)).

$$P_{anc,joint} = \min\,(P_{db} + 0.58.n.P_{anc}\,, 1.58P_{db}\,) \tag{17}$$

Where P_{joint} is the anchored joint capacity, P_{db} is the bond strength, n is the number of anchors and P_{anc} is the anchor capacity as in Eq.(14).

Zhang and Smith 2013 [17] investigated three parameters, which are: plate length after anchor l_{end}, insertion angle of anchor dowel ψ, and FRP fabric width b_f. And provided a combined regression model for multiple anchored joints (see Eq.(18)). Where κ_m is a unified coefficient of three coefficients that considers the three variable parameters.

$$P_{anc.joint} = \alpha\kappa_m P_{db} \tag{18}$$

Cortez Flores et al. 2020 [11] developed an empirical model to estimate the strength of FRP anchored joints (see Eq.(19)), particularly focusing on the influence of various parameters such as reinforcement width, bonded length behind the anchor, and anchor position with respect to the reinforcement. The authors conducted an experimental campaign.

$$P_{anc,joint} = P_{db}. + k_{glob}.P_{anc} \tag{19}$$

Where P_{anc} is the anchor capacity as in Eq.(14) and $k_{glob.}$ is a reduction factor takes into account the anchor position, FRP fabric width, and fan position.

(CNR DT200 R2/2024) [8] provides a design formulation that considers the interaction between the bond strength and anchor strength. This formulation takes the minimum capacity of the bonding plus the anchor capacity or the fabric tensile capacity(see Eq.(20)).

$$P_{anc,joint} = \min(P_{db} \cdot + [n \cdot min\{P_{PO,m},, P_{S,m}, P_{DB,k}, P_{FR,k}\}], P_{t,fabric}) \tag{20}$$

Where P_{db} represents the bond capacity as outlined in CNR DT200 R2/2024. And n is the number of anchors. While P_{po}, P_s,P_{DB}, and P_{FR} the capacities for pull-out dowel sliding, fan sliding, and anchor rupture respectively. Additionally, $P_{t,fabric}$ is the tensile strength of the FRP fabric

In the case of the exterior beam-column strengthening, to determine the number of anchors needed to provide anchorage to the joint fabrics instead of using U-wrapping as shown in Figure 2, CNR DT200 R2/2024 suggests that employing the Eq.(20) by assuming a number of anchors and taking $P_{db}= \varepsilon_{fd}\,.E_f\,.\,A_f$, where ε_{fd} is the effective strain discussed earlier in Eq.(5). And A_f is the fabric area calculated as shown in Eq.(4), but it should exclude the contribution of the fibers aligned with the column axis by omitting the term that accounts for those fibers.

Afterward, recalculate the effective strain ε_{fd} and fabric tensile capacity $p_{t,f}$, ensuring that the total tensile strength of the joint exceeds the required principal tensile stress in Eq.(23).

$$\varepsilon_{fd} = \frac{P_{anc,joint}}{A_f E_f} \tag{21}$$

$$p_{t,f} = \frac{A_f\ E_f\ \varepsilon_{fd}}{b_c\ (h_c/sin\theta)} \tag{22}$$

$$p_{t,tot} = p_{t,c} + p_{t,f}\ \geq\ p_t \tag{23}$$

3 MODEL VALIDATION

The recent experimental campaign conducted by the authors has produced noteworthy results that align closely with the anchored joint capacity defined in Eq. (20) as shown in Figure 3. The specimen tested features two layers of CFRP quadriaxial fabrics, each containing fibers oriented in four directions, with a thickness of 0.053 mm per direction. The fabric has a width (b_f) of 250 mm, a bonded length of 250 mm, and an unbonded length of 50 mm to prevent concrete prism failure.

Furthermore, a CFRP spike anchor with a dowel diameter of 10 mm is positioned at the front of the block, as shown in Figure 3. The depth of anchor embedment (h_{em}) is 110 mm, with a fan length (Ls) of 100 mm, insertion angle (ψ) of 90º, and a fan angle (2λ) of 90º. The tensile strength of the anchor dowel material (f_{FRP}) measures 2512 MPa, while the tensile strength of the CFRP quadriaxial fabrics (f_{frp}) is 3652 MPa. The mean compressive strength of the concrete (f_{cm}) is 24.74 MPa.

$$t_{eff.} = t_f\ .(1 + \frac{2(b_{eff.})}{b_f}.\ cos\theta) \tag{24}$$

By measuring the bonded width of the inclined fibers after failure and analyzing the strain plots across the fabric width using Digital Image Correlation (DIC) for multiple specimens, we determined that the effective width for the inclined fibers b_{eff}, is approximately (0.4 times the total fabric width b_f) for specimens with two layers of CFRP quadriaxial fabric. This relationship can be incorporated into the bond capacity formulation outlined in CNR DT200 R2/2024 by considering the fabric thickness as specified in Eq.(24) where θ represents the angle of inclined fibers in the fabric. Furthermore, this equation excludes the fibers oriented in the perpendicular direction, showcasing a good prediction of the bond capacity for quadriaxial fabrics.

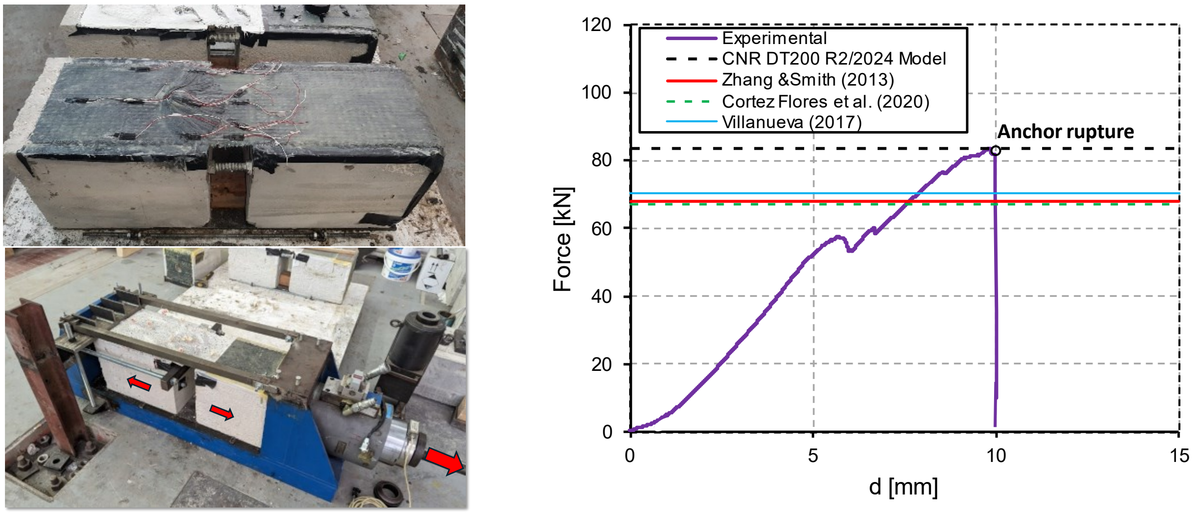

(a) (b)

Figure 3: (a) Tested specimen and test setup; (b) Experimental result.

4 PARAMETRIC STUDY

This parametric study investigates the impact of key design parameters on the capacity of FRP spike anchors as specified by CNR DT 200 R2/2024 [8]. The analysis employs analytical models corresponding to four failure modes: anchor pull-out failure (PO), anchor dowel sliding (S) failure, fan-to-sheet debonding (DB) failure, and anchor fiber rupture (FR) failure. To systematically assess the effect of each parameter, a one-at-a-time (OAT) approach was adopted, where individual parameters—such as anchor embedment depth h_{em}, half of fan angle λ, anchor diameter d_{dowel}, dowel insertion angle ψ, fan length L_s, and concrete strength f_{cm} were varied while keeping other variables constant. This method allowed for a clear evaluation of each parameter's sensitivity and its impact on the predicted anchor capacity across different failure mechanisms. The results are presented through a series of plots Figure 4, illustrating how variations in these parameters influence the load-bearing behavior and governing failure mode, providing valuable insights for optimizing FRP spike anchor design in seismic retrofitting applications.

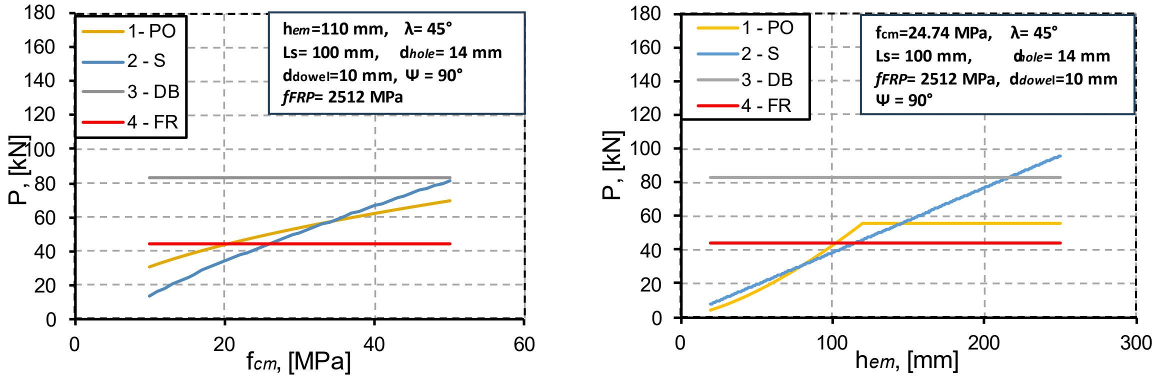

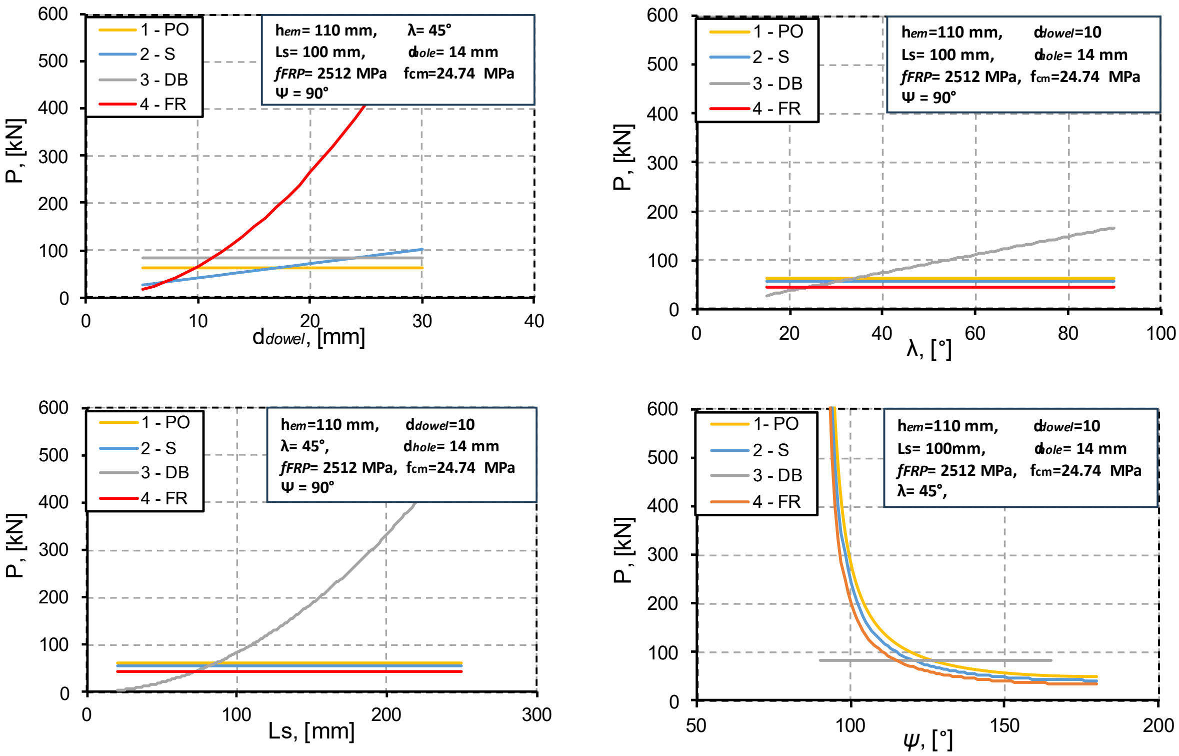

Figure 4: Parametric study

Effect of concrete compressive strength (f_{cm}):

The predicted strength increases with concrete compressive strength *fcm* for the pull-out (PO) and dowel sliding (S) failure modes, showing a linear trend. This indicates that higher concrete strength enhances the anchor capacity for these modes. However, the fan debonding (DB) and anchor rupture (FR) modes exhibit a constant capacity, suggesting that these failure modes are not influenced by the concrete strength within the studied range.

Effect of embedded dowel depth (h_{em}):

The anchor capacity for the dowel sliding (S) mode increases significantly with embedded depth, showing a nearly linear growth, while the Pull-out (PO) mode capacity rises initially before plateauingc, indicating that the maximum effective embedded depth is 120 mm. The fan debonding (DB) and anchor rupture (FR) modes remain unaffected, indicating their failure mechanisms are independent of dowel embedment length. This suggests that increasing the embedded depth *hem* improves performance primarily for shear-related failures.

Effect of dowel diameter (d_{dowel}):

The anchor rupture failure mode (FR) shows a sharp exponential increase in strength with larger dowel diameters, highlighting its critical dependence on dowel size. The dowel sliding (S) mode experiences moderate gain, while the pull-out (PO) and fan debonding (DB) modes remain constant, implying dowel diameter has minimal influence on those modes.

Effect of fan angle (2λ):

The fan debonding failure mode (DB) is highly sensitive to changes in fan angle λ, with capacity increasing significantly as the angle widens. In contrast, other modes (PO, S, FR) show no variation, suggesting that the fan angle primarily affects the fan debonding mechanism.

Effect of fan length *(L_s)*:

The fan debonding failure mode (DB) failure mode again shows a strong positive correlation with fan length Ls, displaying exponential growth in capacity. This indicates that increasing fan length enhances the bonding area, thus improving resistance to fan-sheet debonding. Other failure modes show negligible changes.

Effect of dowel insertion angle (ψ):

Both pull-out (PO), dowel sliding (S), and anchor rupture (FR) failure modes demonstrate a steep decline in capacity as the insertion angle ψ increases, indicating that more vertical dowel orientations significantly reduce anchor strength. The fan debonding failure mode (DB) shows less sensitivity, suggesting their mechanisms are less dependent on dowel orientation.

5 CONCLUSIONS

This study presents an analytical model for predicting the strength of FRP strengthened beam-column joints with spike anchors. By incorporating key influencing parameters such as embedded dowel length, concrete compressive strength, fan angle, dowel insertion angle, and dowel diameter. The proposed model captures the complex interaction mechanisms governing anchor behavior. The analytical predictions align well with an experimental result.

The parametric analysis highlights the sensitivity of anchor strength to geometric and material properties, providing valuable insights for optimizing anchor configurations. Future work will focus on refining the model through extended experimental validation and investigating additional failure modes under dynamic loading conditions. The outcomes of this research contribute to the advancement of FRP anchorage systems, paving the way for more resilient and less disruptive seismic strengthening solutions.

6 ACKNOWLEDGMENTS

This study was performed within the framework of the PE 2024–2026 joint program DPC ReLUIS, WP5 "Integrated and sustainable strengthening interventions for existing constructions". The materials used to strengthen the specimens were provided by Mapei SpA, Milan.

REFERENCES

[1] C. P. Antonopoulos and T. C. Triantafillou, “Experimental Investigation of FRP-Strengthened RC Beam-Column Joints,” *Journal of Composites for Construction*, vol. 7, no. 1, pp. 39–49, Feb. 2003, doi: 10.1061/(asce)1090-0268(2003)7:1(39).

[2] M. Di Ludovico, A. Prota, C. Moroni, G. Manfredi, and M. Dolce, “Reconstruction process of damaged residential buildings outside historical centres after the L’Aquila earthquake: part I—"light damage" reconstruction,” *Bulletin of Earthquake Engineering*, vol. 15, no. 2, pp. 667–692, Feb. 2017, doi: 10.1007/s10518-016-9877-8.

[3] C. Del Vecchio, M. Di Ludovico, A. Balsamo, A. Prota, G. Manfredi, and M. Dolce, “Experimental Investigation of Exterior RC Beam-Column Joints Retrofitted with FRP Systems,” *Journal of Composites for Construction*, vol. 18, no. 4, Aug. 2014, doi: 10.1061/(asce)cc.1943-5614.0000459.

[4] A. Prota, A. Nanni, and G. Manfredi, "Selective upgrade of underdesigned reinforced beam-column joints using carbon fiber-reinforced concrete," 2004. [Online]. Available: https://www.researchgate.net/publication/280016258
[5] S. Pampanin, D. Bolognini, and A. Pavese, "Performance-Based Seismic Retrofit Strategy for Existing Reinforced Concrete Frame Systems Using Fiber-Reinforced Polymer Composites."
[6] M. T. De Risi, C. Del Vecchio, P. Ricci, M. Di Ludovico, A. Prota, and G. M. Verderame, "Light FRP Strengthening of Poorly Detailed Reinforced Concrete Exterior Beam–Column Joints," *Journal of Composites for Construction*, vol. 24, no. 3, Jun. 2020, doi: 10.1061/(asce)cc.1943-5614.0001022.
[7] C. Del Vecchio, M. Di Ludovico, A. Balsamo, and A. Prota, "Minimally Invasive FRP Strengthening of External Beam–Column Joints," *Journal of Composites for Construction*, vol. 28, no. 4, Aug. 2024, doi: 10.1061/JCCOF2.CCENG-4525.
[8] CNR-DT 200/2024, "Guidelines for the Design, Execution, and Control of Static Strengthening Interventions Using Fiber-Reinforced Composites," 2024.
[9] S. Jin Kim and S. T. Smith, "Pullout Strength Models for FRP Anchors in Uncracked Concrete", doi: 10.1061/ASCECC.1943-5614.0000097.
[10] P. Villanueva Llauradó, T. Ibell, J. Fernández Gómez, and F. J. González Ramos, "Pull-out and shear-strength models for FRP spike anchors," *Compos B Eng*, vol. 116, pp. 239–252, May 2017, doi: 10.1016/j.compositesb.2017.02.029.
[11] I. A. Cortez Flores, J. Fernández Gómez, P. Villanueva Llauradó, and A. Ferreira, "An empirical model to estimate FRP anchored joint strength using spike anchors," *Compos Struct*, vol. 254, Dec. 2020, doi: 10.1016/j.compstruct.2020.112789.
[12] E. del Rey Castillo, D. Dizhur, M. Griffith, and J. Ingham, "Strengthening RC structures using FRP spike anchors in combination with EBR systems," *Compos Struct*, vol. 209, pp. 668–685, Feb. 2019, doi: 10.1016/j.compstruct.2018.10.093.
[13] P. Mahrenholtz, J. Y. Cho, J. M. Park, and R. Eligehausen, "Characterization of Shear Strength of FRP Anchors," in *MATEC Web of Conferences*, EDP Sciences, Oct. 2018. doi: 10.1051/matecconf/201819909008.
[14] Stijn. Matthys, *Externally applied FRP reinforcement for concrete structures : technical report*. Fédération internationale du béton, 2019.
[15] C. Del Vecchio, M. Di Ludovico, A. Prota, and G. Manfredi, "Analytical model and design approach for FRP strengthening of non-conforming RC corner beam-column joints," *Eng Struct*, vol. 87, pp. 8–20, Mar. 2015, doi: 10.1016/j.engstruct.2015.01.013.
[16] E. del Rey Castillo, R. Kanitkar, S. T. Smith, M. C. Griffith, and J. M. Ingham, "Design approach for FRP spike anchors in FRP-strengthened RC structures," *Compos Struct*, vol. 214, pp. 23–33, Apr. 2019, doi: 10.1016/j.compstruct.2019.01.100.
[17] H. Zhang and S. T. Smith, "Fibre-reinforced polymer (FRP)-to-concrete joints anchored with FRP anchors: Tests and experimental trends," *Canadian Journal of Civil Engineering*, vol. 40, no. 11, pp. 1103–1116, Sep. 2013, doi: 10.1139/cjce-2012-0525.